



Cite this: DOI: 10.1039/c5gc01237f

## Enhancement of *para*-selectivity in the phenol oxidation with H<sub>2</sub>O<sub>2</sub> over Ti-MCM-68 zeolite catalyst†

S. Inagaki, Y. Tsuboi, M. Sasaki, K. Mamiya, S. Park and Y. Kubota\*

Although titanium silicalite-1 (TS-1) with an **MFI** framework (interconnected 10-ring micropores) is a useful catalyst for phenol oxidation, Ti-MCM-68, a novel **MSE**-type titanosilicate with 12-ring and 10-ring micropores, has been developed as a phenol oxidation catalyst with high activity and selectivity toward the *p*-isomer, hydroquinone. This report describes the improvement in catalytic activity and *para*-selectivity of Ti-MCM-68 for phenol oxidation. Thermal treatment after Ti insertion significantly enhanced the catalytic activity of Ti-MCM-68, mainly due to an improvement in the hydrophobicity in the micropores. Silylation of the external surface of Ti-MCM-68 with Ph<sub>2</sub>SiCl<sub>2</sub>, followed by Ti insertion and calcination, showed greater *para*-selectivity, indicating that the selective formation of *p*-isomers occurred within one-dimensional 12-ring micropores in the Ti-MCM-68. The addition of ethanol as a cosolvent to the reaction mixture resulted in the best *para*-selectivity (>94%) and activity among the modified Ti-MCM-68 catalysts.

Received 7th June 2015,  
Accepted 20th August 2015

DOI: 10.1039/c5gc01237f

www.rsc.org/greenchem

## Introduction

Partial oxidation reactions are important for the production of practical and functional chemicals. In conventional oxidation processes, powerful oxidizing agents, such as KMnO<sub>4</sub>, NaClO<sub>3</sub>, CrO<sub>3</sub>, *m*-chloroperoxybenzoic acid (MCPBA), peracetic acid and other peroxycarboxylic acids/alkyl hydroperoxides, are utilized. For example, hydroquinone (HQ), a key intermediate in the manufacture of polymeric materials, *e.g.*, PEEK (poly[ether ether ketone]) resin, is produced *via* the oxidation of aniline (with stoichiometric quantities of MnO<sub>2</sub> and H<sub>2</sub>SO<sub>4</sub>) to *p*-benzoquinone, followed by reduction through stoichiometric consumption of Fe and H<sub>2</sub>O (see the ESI, Fig. S1†).<sup>1</sup> This process is not environmentally friendly because the production of HQ is accompanied by the formation of one equivalent of (NH<sub>4</sub>)<sub>2</sub>SO<sub>4</sub> and FeO as well as four equivalents of MnSO<sub>4</sub>. Alternatively, a novel environmentally benign route has been developed by Upjohn.<sup>1</sup> This newer route consists of bisphenol-A synthesis starting with two equivalents of phenol and one equivalent of acetone, followed by heterolytic cracking of the

bisphenol-A into *p*-isopropenylphenol and phenol, and oxidation of *p*-isopropenylphenol into HQ with the simultaneous formation of acetone (Fig. S1†). The phenol and acetone (formed during the process as coproducts) can be used as the starting materials. In addition, no significant quantity of salt waste is formed. This is a typical “green” chemical process; however, more straightforward routes to the desired product of HQ warrant investigation.

Hydrogen peroxide (H<sub>2</sub>O<sub>2</sub>) is a preferable oxidant for environmentally benign liquid-phase reactions because it can oxidize organic compounds with an atom efficiency of 47% and with the generation of water as the only coproduct, theoretically. Since titanium-substituted molecular sieves with isolated tetrahedral Ti species in the zeolite framework are required for selective oxidation reactions with H<sub>2</sub>O<sub>2</sub>,<sup>2–6</sup> a variety of titanosilicate catalysts, such as TS-1,<sup>7</sup> TS-2,<sup>8</sup> Ti-beta (Ti-BEA),<sup>9–11</sup> Ti-ZSM-12 (Ti-MTW),<sup>12</sup> Ti-ZSM-48,<sup>13</sup> Ti-mordenite (Ti-MOR),<sup>14</sup> Ti-SSZ-33,<sup>15</sup> Ti-ITQ-7 (Ti-ISV),<sup>16</sup> Ti-SSZ-23 (Ti-STT)<sup>17</sup> and Ti-MCM-22 (Ti-MWW),<sup>18–21</sup> have been developed for “green” and sustainable chemical processes.

Titanium silicalite-1 (TS-1) with **MFI** topology (10 × 10-membered rings) is an industrially useful titanosilicate, which is effective for phenol oxidation with H<sub>2</sub>O<sub>2</sub> to HQ and catechol (CL) (Fig. S1†). Up to 85% *para*-selectivity has been achieved through post-synthetic modification of TS-1 or with the aid of a solvent in the reaction.<sup>22–24</sup> Recently, Ti-MCM-68<sup>25</sup> and Ti-YNU-2<sup>26</sup> have been developed as phenol oxidation catalysts with high activity and selectivity toward hydroquinone. These are novel **MSE**-type titanosilicates with a 12 × 10 × 10R pore

Division of Materials Science and Chemical Engineering, Yokohama National University, 79-5 Tokiwadai, Hodogaya-ku, Yokohama 240-8501, Japan.

E-mail: kubota@ynu.ac.jp

† Electronic supplementary information (ESI) available: Detailed preparation procedures of catalysts, textural properties, reaction pathways, schematic diagram of the preparation of Ti-MCM-68, graphics for size-comparison, schemes for plausible mechanism of phenol oxidation, and results of FT-IR, <sup>13</sup>C CP MAS NMR, TG-DTA, and N<sub>2</sub>-adsorption. See DOI: 10.1039/c5gc01237f

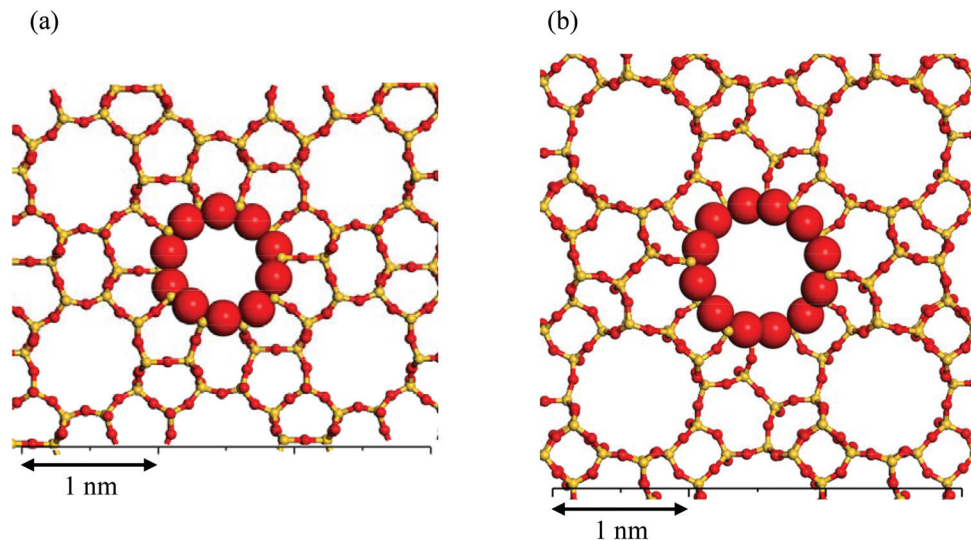


Fig. 1 Projections of the (a) 10R window ( $0.51 \times 0.55$  nm) in TS-1 (MFI viewed along [010]) and (b) 12R window ( $0.64 \times 0.68$  nm) in Ti-MCM-68 (MSE viewed along [001]). The ionic radii of oxygen (red) and silicon (orange) in the center of each figure are 0.135 and 0.04 nm, respectively.

system in which a 12R straight channel intersects with two twisted 10R channels.<sup>27</sup> These materials also contain a large cavity ( $18 \times 12R$ ) accessible only through the 10R pores. As shown in Fig. 1a, the crystallographic dimensions of the 10R window of the straight channel in TS-1 (MFI) were  $0.51 \times 0.55$  nm when the ionic radii of  $O^{2-}$  and  $Si^{4+}$  were defined as 0.135 and 0.04 nm, respectively.<sup>28</sup> Although breathing of the pore window could make the aperture expand momentarily, diffusion of a phenol molecule into the 10R straight channel of TS-1 was limited. In contrast, a 12R aperture in Ti-MCM-68 (MSE),  $0.64 \times 0.68$  nm (Fig. 1b),<sup>28</sup> is wide enough to allow a phenol molecule to enter. Therefore, Ti-MCM-68 is a promising catalyst for selective *p*-hydroquinone production with high efficiency for phenol oxidation.

The MSE-type molecular sieves can be obtained hydrothermally only as an aluminosilicate, and the Si/Al molar ratio of the product is limited to the range of 9–12.<sup>29–32</sup> While Al-MCM-68 can be synthesized using *N,N,N',N'*-tetraethylbicyclo[2.2.2]oct-7-ene-2,3:5,6-dipyrrolidinium diiodide (TEBOP<sup>2+</sup>(I<sup>-</sup>)<sub>2</sub>) or another quaternary ammonium cation as a structure-directing agent (SDA),<sup>33</sup> researchers<sup>34</sup> have reported the synthesis of an UZM-35 zeolite, which has topology identical to MSE, but can be synthesized using dimethyldipropylammonium hydroxide as the SDA. Recently, a wide variety of MSE-type aluminosilicates were developed during hydrothermal conversion of zeolite Y (FAU)<sup>35</sup> or *via* seed-assisted crystallization under OSDA-free synthetic conditions.<sup>36,37</sup> A precursor of the pure silica version of the MSE topology (YNU-2P) and its stabilized microporous version (YNU-2)<sup>26,38</sup> have been synthesized by utilizing the steam-assisted crystallization (SAC) method.<sup>39</sup>

Conversely, for the titanosilicate version, direct crystallization of Ti-MSE remained difficult using any of the methods effective for aluminosilicates or pure-silica materials. One option for introducing a sufficient amount of Ti into the

framework was isomorphous substitution of conventional Al-MCM-68 to Ti-MCM-68, which was accomplished using post-synthetic modification of Al-MCM-68 (dealumination by acid treatment followed by gas-phase Ti insertion using  $TiCl_4$  as the Ti source, see Fig. S2†).<sup>25</sup> The present report describes the improvement in catalytic activity and *para*-selectivity of Ti-MCM-68 for phenol oxidation, and the effects of post-synthetic silylation of external site defects and the addition of a cosolvent on catalytic performance.

## Results and discussion

### Catalyst preparation

Fig. 2 shows powder XRD patterns of the as-synthesized sample and the post-synthetically treated samples. The as-synthesized product possessed an MSE framework without any impure phases, and after subsequent calcination and acid treatment, the framework structures remained unchanged. Acid treatment successfully produced highly dealuminated MCM-68 (Si/Al > 1000, determined by ICP-AES analysis), likely including some site defects (vacancy defects) in the MSE framework. During  $TiCl_4$  treatment at 600 °C, the Ti species was inserted into the site defects of dealuminated MCM-68, which was confirmed by the sole presence of the UV-Vis peak at *ca.* 210 nm (Fig. 3), corresponding to 4-coordinated Ti species in the silicate framework. Other possible peaks corresponding to 5- or 6-coordinated Ti species would appear at around 250–290 nm, which are not observed in Fig. 3 but discussed elsewhere.<sup>5,26</sup> It should be noted that the dealuminated MCM-68 free of Ti atoms gave no obvious UV-vis peaks (Fig. 3a). Another sign of Ti-incorporation into the framework is the presence of a characteristic IR band at around  $960\text{ cm}^{-1}$  (Fig. S3†), which is consistent with earlier examples.<sup>40,41</sup> The

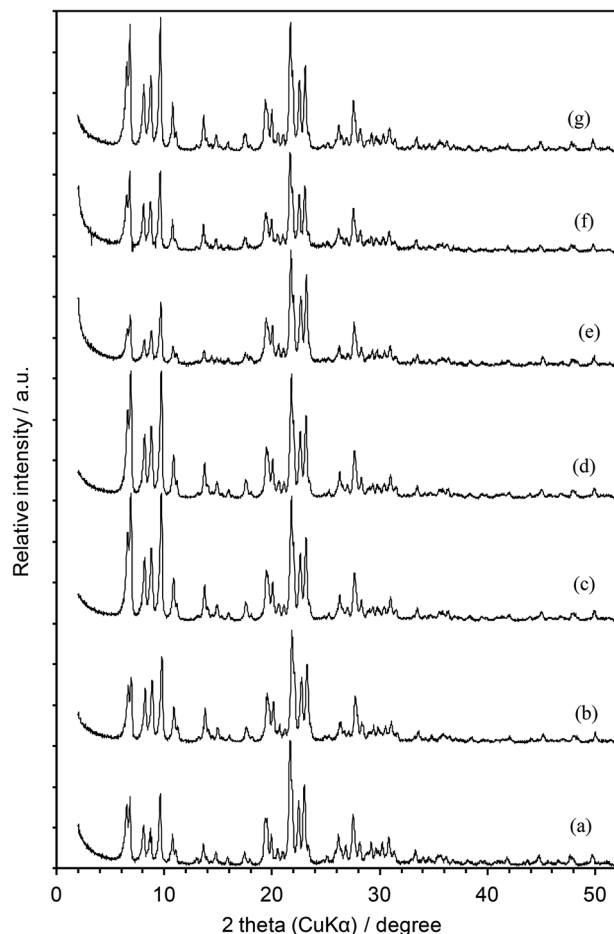


Fig. 2 XRD patterns of (a) calcined Al-MCM-68, (b) dealuminated MCM-68, (c) Ti-MCM-68, (d) Ti-MCM-68\_cal, (e) Ph<sub>2</sub>Si-MCM-68, (f) Ph<sub>2</sub>Si/Ti-MCM-68, and (g) Si/Ti-MCM-68\_cal.

Ti contents of both Ti-MCM-68 and its calcined version (Ti-MCM-68\_cal) were *ca.* 0.24 mmol g<sup>-1</sup> (Table 1).

The Ph<sub>2</sub>SiCl<sub>2</sub> treatment of dealuminated MCM-68 gave Ph<sub>2</sub>Si-modified MCM-68 with *ca.* 0.1 mmol g<sup>-1</sup> Ph<sub>2</sub>Si on the surface (*ca.* 1.1 molecules per nm<sup>2</sup>), as confirmed by <sup>13</sup>C MAS NMR and TG-DTA analyses (Fig. S4 and S5,† respectively). In the <sup>13</sup>C CP MAS NMR, two peaks at 133.9 and 137.9 ppm were assigned to the phenyl group in Ph<sub>2</sub>Si on the MCM-68 surface; the peaks at 128.4, 124.8 and 20.2 ppm were assigned to toluene, which was a residue after silylation. In the TG-DTA, a decrease in weight (8.1 wt%) at the lower temperature (from room temperature to *ca.* 100 °C) was caused by desorption of water, toluene and adsorbed molecules, and a typical decrease (1.5 wt%) at around 300 °C occurred due to combustion of the phenyl group immobilized on the surface of dealuminated MCM-68. The Ph<sub>2</sub>SiCl<sub>2</sub> molecules that were larger than the 12R micropores (see Fig. S6†) could react selectively with the silanols at the external site defects of dealuminated MCM-68. The subsequent TiCl<sub>4</sub> treatment of Ph<sub>2</sub>Si-modified MCM-68 successfully allowed Ti insertion in site defects located on the micropore surface, which was supported by the appearance of

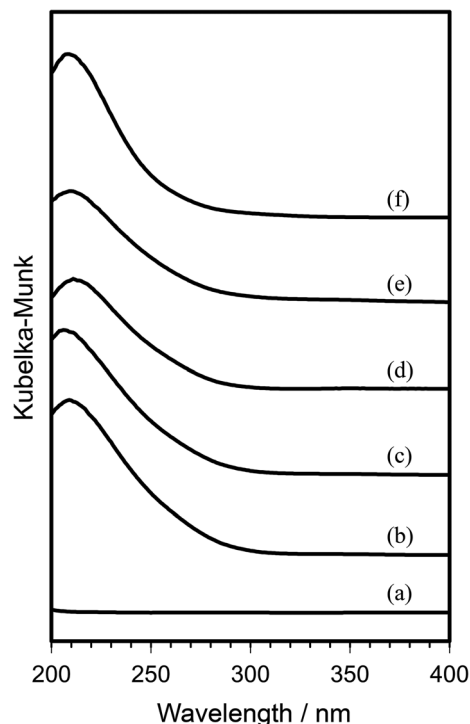


Fig. 3 DR UV-vis spectra of (a) deAl-MCM-68, (b) Ti-MCM-68, (c) Ti-MCM-68\_cal, (d) Ph<sub>2</sub>Si-Ti-MCM-68, (e) Si/Ti-MCM-68\_cal, and (f) TS-1.

a UV-Vis peak at *ca.* 210 nm (Fig. 3). After the combustion of the phenyl groups by calcination of Ph<sub>2</sub>Si-Ti-MCM-68 at 650 °C, the Ti content of the calcined sample (Si/Ti-MCM-68\_cal) was 0.3 mmol g<sup>-1</sup>, very similar to Ti-MCM-68\_cal (0.24 mmol g<sup>-1</sup>), indicating that TiCl<sub>4</sub> molecules penetrated into the micropores within Ph<sub>2</sub>Si-MCM-68, independent of the phenyl groups situated on the external surface.

FE-SEM observations (Fig. 4) indicated that all of the MCM-68 samples were tiny particles (50–100 nm) and that TS-1 consisted of agglomerates (*ca.* 300 nm) of tiny particles (50–100 nm). The nitrogen adsorption–desorption isotherms (Fig. S7†) indicated that Ti-MCM-68, Ti-MCM-68\_cal and Si/Ti-MCM-68\_cal had similar BET surface areas (*ca.* 500 m<sup>2</sup> g<sup>-1</sup>) and micropore volumes (0.19–0.20 cm<sup>3</sup> g<sup>-1</sup>). Calcination of Ti-MCM-68 at 650 °C improved hydrophobicity, as confirmed by the water adsorption isotherm (Fig. 5). The hydrophobicity of Si/Ti-MCM-68\_cal was moderate, and was between that of Ti-MCM-68 and Ti-MCM-68\_cal. <sup>29</sup>Si MAS NMR and FT-IR indicated the decrease in (SiO)<sub>3</sub>SiOH (Q<sup>3</sup>) peaks and silanols (isolated and hydrogen-bonded species), respectively (not shown).

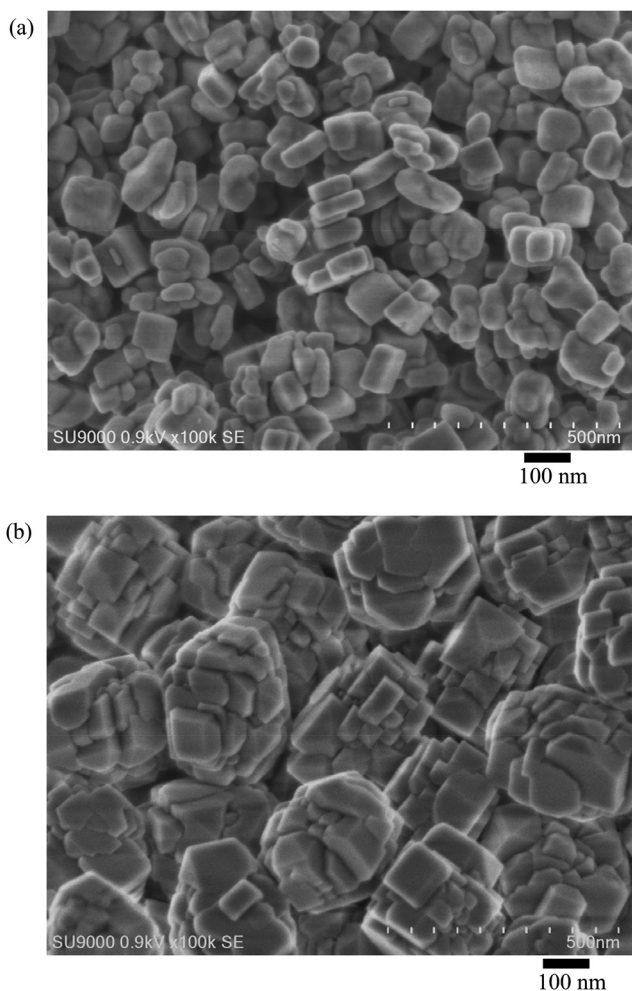
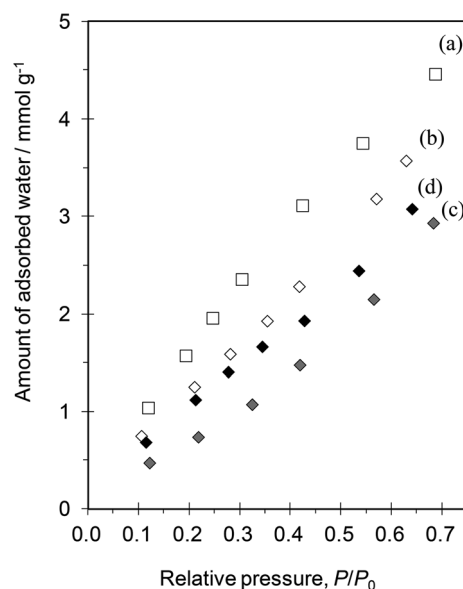
### Improvement in *para*-selectivity

Table 1 lists the results of phenol oxidation with H<sub>2</sub>O<sub>2</sub> on titanosilicate catalysts prepared for this study. First, the catalytic performance of titanosilicates was investigated under conditions in which water from the H<sub>2</sub>O<sub>2</sub> solution and an excess of phenol were the reaction media. No *meta* isomer (resorcinol) was detected and no interconversion was observed

**Table 1** Oxidation of phenol with H<sub>2</sub>O<sub>2</sub> catalyzed by various titanasilicates

Catalyst	Ti content <sup>a</sup> (mmol g <sup>-1</sup> )	Cosolvent	TON <sup>b</sup>	Yield <sup>c</sup> (%)				
				Total	HQ <sup>d</sup>	CL <sup>d</sup>	<i>p</i> -BQ <sup>d</sup>	<i>para</i> -Sel. <sup>e</sup> (%)
Ti-MCM-68	0.235	None	90	10.0	6.5	3.5	0.0	65.0
		MeOH	75	8.1	5.9	0.4	1.8	95.1
		EtOH	134	15.2	14.0	1.2	0.0	92.0
		MeCN	118	13.1	9.4	2.9	0.9	78.3
Ti-MCM-68_cal	0.241	None	314	35.0	26.3	7.6	1.2	78.3
		MeOH	324	35.9	33.1	2.8	0.0	92.2
		EtOH	446	49.2	45.8	3.4	0.0	93.1
		MeCN	419	47.4	39.0	5.5	2.9	88.4
Si/Ti-MCM-68_cal	0.300	None	259	35.7	28.3	6.5	1.0	81.9
		MeOH	335	46.7	42.9	3.4	0.0	92.7
		EtOH	651	82.3	77.6	4.6	0.0	94.4
		MeCN	460	65.3	56.3	6.3	2.7	90.3
TS-1	0.373	Neat	90	15.2	8.6	6.6	0.0	56.8
		MeOH	32	5.7	4.3	1.4	0.0	75.3
		EtOH	27	4.8	3.5	1.4	0.0	71.9
		MeCN	47	8.1	4.0	4.2	0.0	48.7

Reaction conditions: catalyst, 20 mg; phenol, 21.25 mmol; H<sub>2</sub>O<sub>2</sub> (31 wt%), 4.25 mmol; H<sub>2</sub>O, 17.8 mmol; cosolvent, 4.0 g; temperature, 70 °C; time, 60 min. <sup>a</sup> Determined by ICP analysis. <sup>b</sup> Turnover number (moles of [HQ + CL + *p*-BQ] per mole of Ti site). <sup>c</sup> Product yields based on added H<sub>2</sub>O<sub>2</sub> after exhaustive acetylation of the products with excess Ac<sub>2</sub>O–K<sub>2</sub>CO<sub>3</sub>, the derivatized products were analyzed by GC (0.25 mm × 30 m × 1.00 μm DB-1 column, internal standard: anisole, detector: FID). <sup>d</sup> HQ = hydroquinone, CL = catechol, *p*-BQ = *p*-benzoquinone. <sup>e</sup> Selectivity to *para*-isomers of dihydroxybenzenes and quinones (moles of [HQ + *p*-BQ] per mole of [HQ + CL + *p*-BQ]).

**Fig. 4** Typical FE-SEM images of (a) Ti-MCM-68 and (b) TS-1.**Fig. 5** H<sub>2</sub>O adsorption isotherms at 298 K of (a) TS-1, (b) Ti-MCM-68, (c) Ti-MCM-68\_cal, and (d) Si/Ti-MCM-68\_cal.

between HQ and CL in independent experiments. The total yield in Ti-MCM-68\_cal (35.0%) was significantly greater than that in Ti-MCM-68 (10.0%), which agreed well with a previous report.<sup>25</sup> Water adsorption isotherm measurements (Fig. 5) suggested that this improvement in catalytic activity was due to an increase in hydrophobicity. The Si/Ti-MCM-68\_cal also showed a high total yield (35.7%) comparable to Ti-MCM-68\_cal (35.0%), strongly suggesting that tetrahedral Ti species

were successfully formed in the MSE framework during  $\text{TiCl}_4$  treatment, regardless of  $\text{Ph}_2\text{SiCl}_2$  pre-treatment.

All three Ti-MCM-68 catalysts possessed greater *para*-selectivity compared to TS-1 (56.8%). The greater *para*-selectivity in Ti-MCM-68\_cal (78.3%) compared to that in Ti-MCM-68 (65.0%) was probably caused by the predominant shape-selective reaction in the hydrophobic micropores to give *p*-isomers. Wilkenhöner *et al.*<sup>22</sup> suggested two possible reaction mechanisms (A and B) for the formation of CL (*o*-isomer) during phenol oxidation over TS-1; mechanism A involves a phenol molecule coordinated to Ti-peroxo species that was transformed into CL through a penta-coordinate trigonal bipyramidal Ti site; mechanism B involves the formation of CL without coordination of phenol to the active titanium site, which occurred *via* a six-membered ring transition state involving phenol. Both mechanisms indicate that, for less restricted geometric Ti sites (as on the external surface of TS-1), CL is the preferred product. Conversely, the formation of *p*-isomer, HQ, can be assisted neither by coordination nor by a six-membered ring transition state. It should be formed in a shape-selective way under limiting geometrical conditions, as in the suitable micropores. The 10R pores of TS-1 ( $0.51 \times 0.55$  nm) are a little too small to show sufficient shape-selectivity. Thus, in the liquid-phase reaction, the 12R micropores ( $0.64 \times 0.68$  nm) in Ti-MCM-68 may efficiently promote a restricted geometry, leading to selective formation of hydroquinone. The above-mentioned mechanism B could be partially applicable to the present case by removing the assistance of a six-membered ring transition state but with the aid of steric restriction by a suitable 12R micropore, as shown in Fig. S8.† The slightly wider pores in Ti-MCM-68 dramatically enhanced the diffusivity of phenol molecules while maintaining the restricted geometry inside the pore, causing the *para*-selective reaction predominantly compared to the relatively narrow micropores of TS-1. Intracrystalline diffusivity of phenol in Ti-beta (12R,  $0.66 \times 0.67$  nm) was much greater ( $D = 3.9 \times 10^{-16} \text{ m}^2 \text{ s}^{-1}$ ) than that in TS-1 ( $D = 5.2 \times 10^{-17} \text{ m}^2 \text{ s}^{-1}$ ) at 30 °C in water.<sup>23</sup> This can explain the much greater *para*-selectivity over Ti-MCM-68 catalysts. Note that Si/Ti-MCM-68\_cal gave excellent *para*-selectivity (81.9%), suggesting that  $\text{Ph}_2\text{SiCl}_2$  molecules reacted with the site defects on the external surface of dealuminated MCM-68, while  $\text{TiCl}_4$  molecules selectively reacted with the site defects on the micropore surface.

### Effect of cosolvent

In the TS-1 catalyst system, *para*-selectivity improved from 56% to 68% when methanol (MeOH) was added as a cosolvent to the reaction mixture.<sup>22</sup> One possible reason proposed was that the coordination of the protic solvent increases the size of the active Ti site. In the narrow TS-1 micropores, this coordination provides geometric constraints for an approaching phenol molecule. Therefore, phenol will approach the bulky Ti site with the OH group pointing away from the Ti site, producing HQ.<sup>22</sup> The effect of a cosolvent in the Ti-MCM-68 system for phenol oxidation was also investigated.

Table 1 lists typical results for phenol oxidation over titanosilicate catalysts upon the addition of MeOH, ethanol (EtOH) or acetonitrile (MeCN) as a cosolvent. No oxidation products of EtOH, such as acetaldehyde (MeCHO) and/or acetic acid (AcOH), were detected in this reaction system. When MeOH or EtOH was added to the TS-1 system, the total yield of the products greatly decreased even though *para*-selectivity was slightly improved. This improvement may have been caused by lower opportunity of *o*-hydroxylation on the external surface due to the covering of external tetrahedral Ti sites with alcohols. As an additional factor, the presence of alcohols inside 12-ring micropores might cause a little more steric restriction forcing *para*-substitution to occur. Meanwhile, the addition of MeCN in the TS-1 system decreased the total yield as well as *para*-selectivity.

In contrast, in all three Ti-MCM-68 systems, a dramatic improvement of catalytic activity and *para*-selectivity occurred upon the addition of a cosolvent. For example, the addition of EtOH in the Si/Ti-MCM-68\_cal system resulted in 82.3% total yield and 94.4% *para*-selectivity. The relative hydrophilicity of Ti-MCM-68 (Fig. 5) makes the hydrogen bonding of MeOH or EtOH with Si-OH in the external surface of catalysts more likely, narrowing the pore mouth and covering external active Ti sites. Therefore, Ti-MCM-68 in MeOH or EtOH exhibited greater *para*-selectivity at relatively lower catalytic activity, compared to neat (cosolvent-free) conditions. The more hydrophobic Ti-MCM-68\_cal containing only a trace amount of external Si-OH groups could interact with a lower amount of MeOH or EtOH, resulting in a much more hydrophobic external surface, without pore narrowing, that helped guide phenol molecules into the 12R micropores and to allow shape-selective reactions to occur. These factors may have improved the catalytic activity and greater *para*-selectivity for phenol oxidation over Ti-MCM-68\_cal in the presence of a cosolvent. For Si/Ti-MCM-68\_cal, the addition of EtOH improved both the catalytic activity and *para*-selectivity compared to MeOH addition, probably due to the greater hydrophobicity of the ethyl group compared to the methyl group on the external surface of titanosilicate particles. When isopropyl alcohol (*i*-PrOH) was added as a cosolvent to the reaction system, Si/Ti-MCM-68\_cal produced a total yield of 65% with greater *para*-selectivity (93%), indicating that isopropyl groups on the external surface were hydrophobic enough to guide phenol into the micropores, but were too bulky to allow easy access of a phenol molecule into the 12R-pore. This tendency was also observed for Ti-MCM-68 and Ti-MCM-68\_cal. Consequently, EtOH addition could improve both the catalytic activity and *para*-selectivity of the Ti-MCM-68 catalyst for phenol oxidation, probably due to enhancement of hydrophobicity *via* covering of external Ti sites and Si-OH with EtOH. Although MeCN also appears to be a good cosolvent for improving the hydrophobicity of the external surface of Ti-MCM-68, the MeCN molecules may interact more strongly with active Ti sites located on the micropore surface and deactivate the catalytic active sites during phenol oxidation.

## Experimental

### Preparation of titanosilicates

Ti-MCM-68 was prepared from Al-MCM-68 through dealumination by nitric acid treatment,  $\text{TiCl}_4$  treatment and calcination.<sup>25,30–33</sup> The detailed synthetic procedure of Ti-MCM-68 is available in the ESI.† However, for this study, an alternative synthetic route to Ti-MCM-68 was developed to insert the Ti species into internal site defects selectively. In a typical procedure, the silylation of external site defects of dealuminated MCM-68 (1.0 g) with  $\text{Ph}_2\text{SiCl}_2$  (0.2 g) was conducted under reflux conditions for 24 h in toluene (50 mL), followed by recovery of the silylated solid through filtration and drying at room temperature. Next, the  $\text{Ph}_2\text{Si}$ -modified sample was exposed to a flow of argon bubbled through a vessel containing  $\text{TiCl}_4$ . The  $\text{TiCl}_4$  flow was continued for 60 min at 600 °C. The resulting Ti- $\text{Ph}_2\text{Si}$ -MCM-68 was treated thermally at 650 °C for 4 h in a furnace to give Si/Ti-MCM-68\_cal.

TS-1 was obtained from the Asia Catalyst Project in collaboration with the Catalysis Society of Japan as an Asia-reference catalyst TS-1 (catalogue specification: Si/Ti = 35).

### Characterization

All titanosilicates used in this study were characterized by powder X-ray diffraction (XRD, Ultima-IV, Rigaku) using  $\text{CuK}\alpha$  radiation at 40 kV and 20 mA. The textural properties, specific surface area and micropore volume of titanosilicates were evaluated using the nitrogen adsorption–desorption isotherm (BELSORP-max-1-N, Bel Japan) at 77 K. The morphologies of zeolite catalysts were observed by field emission scanning electron microscopy (FE-SEM, SU9000, Hitachi). The contents of Ti in titanosilicates were measured using inductively coupled plasma atomic emission spectrometry (ICP-AES, ICPE-9000, Shimadzu). The coordination states of Ti species in the titanosilicates were evaluated using diffuse reflectance UV-vis spectroscopy (DR/UV-Vis, V-550 spectrometer, JASCO). The organic contents in  $\text{Ph}_2\text{Si}$ -modified materials were measured using thermogravimetry (Thermo-Plus, Rigaku).

The FT-IR spectra of titanosilicates were recorded on a JASCO FT/IR-6100 spectrometer equipped with a TGS detector. A titanosilicate sample (*ca.* 1 mg) diluted with KBr powder (*ca.* 100 mg) was used for the measurement in the region of 700–1000  $\text{cm}^{-1}$ .

The solid-state magic angle spinning nuclear magnetic resonance (MAS NMR) spectra were obtained using an AVANCEIII 600 (Bruker) instrument operating at 600 MHz for  $^1\text{H}$  and 150 MHz for  $^{13}\text{C}$ . All of the MAS NMR spectra were obtained at room temperature in a 4 mm diameter  $\text{ZrO}_2$  tube. The  $^{13}\text{C}$  chemical shifts were determined using glycine. The cross-polarization (CP) MAS NMR measurements were obtained using 2000 pulses with a recycle time of 4.0 s at a spinning rate of 10 kHz.

### Reaction procedures

The oxidation of phenol with  $\text{H}_2\text{O}_2$  was performed as follows. Catalyst (20 mg), phenol (2.00 g, 21.25 mmol) and a 31 wt%

aqueous solution of  $\text{H}_2\text{O}_2$  (466 mg, 4.25 mmol) were loaded into a 35 mL glass pressure tube. When the cosolvent was used, 4.0 g of MeOH, EtOH, *i*-PrOH, or MeCN was added to the reaction mixture. The whole mixture was immediately immersed in a pre-heated oil bath to start the reaction. The reaction mixture was stirred at 70 °C for 60 min, and then immediately cooled in an ice bath to stop the reaction. Sulfolane (2.0 g as a suitable unreactive solvent for derivatization), anisole (225 mg, 2.0 mmol, as an internal standard), and the catalyst was removed from the reaction mixture by centrifugation. The supernatant (100 mg) was treated with an excess amount of acetic anhydride (*ca.* 200 mg, 2 mmol) and  $\text{K}_2\text{CO}_3$  (*ca.* 300 mg) at 35 °C for 10 min to achieve exhaustive acetylation of the phenolic OH groups. After removing the residual inorganic solids by filtration through a membrane filter and adjusting the concentration to the one suitable for gas chromatography (GC) with chloroform, the GC analysis was performed on a Shimadzu GC-2014 instrument equipped with a flame ionization detector using a capillary column of DB-1 (30 m length, 0.25 mm diameter, and 1.00  $\mu\text{m}$  film thickness). The unreacted  $\text{H}_2\text{O}_2$  was quantified using the iodometry method involving titration of a well-stirred solution of the reaction mixture (1.0 g) and KI (0.2 g) in 2.0 mol  $\text{L}^{-1}$  hydrochloric acid (50 mL) with 0.1 mol  $\text{L}^{-1}$  aqueous  $\text{Na}_2\text{S}_2\text{O}_3$  solution.

## Conclusions

The Ti-MCM-68 catalyst with an MSE structure demonstrated greater catalytic activity and *para*-selectivity for phenol oxidation with  $\text{H}_2\text{O}_2$  compared to the conventional catalyst TS-1 with an MFI structure. The high *para*-selectivity of Ti-MCM-68 was due to the predominant shape-selective reaction in hydrophobic 12R micropores to give *p*-isomers, unlike the behaviour of the 10R micropores in TS-1. The high catalytic activity of Ti-MCM-68 was caused by the high diffusivity of phenol within the 12R channels. Thermal treatment after Ti-insertion significantly enhanced the catalytic activity of Ti-MCM-68, due mainly to an increase in the hydrophobic nature inside the pores. Note that Si/Ti-MCM-68 showed greater *para*-selectivity for phenol oxidation in the presence of EtOH as a cosolvent. The high *para*-selectivity (>94%) of Si/Ti-MCM-68\_cal while maintaining a high turnover number (TON) is considered to be due to enhancement of hydrophobicity by covering external Ti sites through Si–OH and EtOH interactions.

## Acknowledgements

This work was financially supported in part by Grants-in-Aid for Scientific Research (no. 13199071 and 23760741) from the Japan Society for the Promotion of Science (JSPS). We are grateful to Prof. T. Tatsumi of Tokyo Institute of Technology for helpful discussion. We thank Dr A. Endo of National Institute of Advanced Industrial Science and Technology and Mr Y. Ohno of Yokohama National University for technical assistance.

## Notes and references

- 1 J. H. Clark, *Green Chem.*, 1999, **1**, 1.
- 2 B. Notari, *Adv. Catal.*, 1996, **41**, 253.
- 3 T. Tatsumi, *Curr. Opin. Solid State Mater. Sci.*, 1997, **2**, 76.
- 4 I. W. C. E. Arends and R. A. Sheldon, *Appl. Catal., A*, 2001, **212**, 175.
- 5 P. Ratnasamy, D. Srinivas and H. Knözinger, *Adv. Catal.*, 2004, **48**, 1.
- 6 P. Wu and T. Tatsumi, *Catal. Surv. Asia*, 2004, **8**, 137.
- 7 M. Taramasso, G. Perego and B. Notari, *US Pat*, 1983, 4410501.
- 8 J. S. Reddy, R. Kumar and P. Ratnasamy, *Appl. Catal.*, 1990, **58**, L1.
- 9 M. A. Cambor, A. Corma, A. Martínez and J. Pérez-Pariente, *J. Chem. Soc., Chem. Commun.*, 1992, 589.
- 10 J. C. van der Waal, P. J. Kooyman, J. C. Jansen and H. Van Bekkum, *Microporous Mesoporous Mater.*, 1998, **25**, 43.
- 11 T. Tatsumi and N. Jappari, *J. Phys. Chem.*, 1998, **102**, 7126.
- 12 A. Tuel, *Zeolites*, 1995, **15**, 236.
- 13 D. P. Serrano, H.-X. Li and M. E. Davis, *J. Chem. Soc., Chem. Commun.*, 1992, 745.
- 14 P. Wu, T. Komatsu and T. Yashima, *J. Phys. Chem.*, 1996, **100**, 10316.
- 15 C. B. Dartt and M. E. Davis, *Appl. Catal., A*, 1996, **143**, 53.
- 16 M.-J. Díaz-Cabanás, L. A. Villaescusa and M. A. Cambor, *Chem. Commun.*, 2000, 761.
- 17 E. A. Eilertsen, F. Giordanino, C. Lamberti, S. Bordiga, A. Damin, F. Bonino, U. Olsbye and K. P. Lillerud, *Chem. Commun.*, 2011, **47**, 11867.
- 18 P. Wu, T. Tatsumi, T. Komatsu and T. Yashima, *J. Phys. Chem. B*, 2001, **105**, 2897.
- 19 P. Wu and T. Tatsumi, *Chem. Commun.*, 2002, 1026.
- 20 P. Wu, T. Miyaji, Y. Liu, M. He and T. Tatsumi, *Catal. Today*, 2005, **99**, 233.
- 21 P. Wu, D. Nuntasri, J. Ruan, Y. Liu, M. He, W. Fan, O. Terasaki and T. Tatsumi, *J. Phys. Chem. B*, 2004, **108**, 19126.
- 22 U. Wilkenhöner, G. Langhendries, F. van Laar, G. V. Baron, D. W. Gammon, P. A. Jacobs and E. van Steen, *J. Catal.*, 2001, **203**, 201.
- 23 U. Wilkenhöner, W. L. Duncan, K. P. Möller and E. van Steen, *Microporous Mesoporous Mater.*, 2004, **69**, 181.
- 24 T. Yokoi, P. Wu and T. Tatsumi, *Catal. Commun.*, 2003, **4**, 11.
- 25 Y. Kubota, Y. Koyama, T. Yamada, S. Inagaki and T. Tatsumi, *Chem. Commun.*, 2008, 6224.
- 26 M. Sasaki, Y. Sato, Y. Tsuboi, S. Inagaki and Y. Kubota, *ACS Catal.*, 2014, **4**, 2653.
- 27 D. L. Dorset, S. C. Weston and S. S. Dhingra, *J. Phys. Chem. B*, 2006, **110**, 2045.
- 28 Ch. Baerlocher, L. B. McCusker and D. H. Olson, *Atlas of Zeolite Framework Types*, Elsevier, Amsterdam, 6th edn, 2007, see also: <http://www.iza-structure.org/databases>.
- 29 D. C. Calabro, J. C. Cheng, R. A. Crane Jr., C. T. Kresge, S. S. Dhingra, M. A. Steckel, D. L. Stern and S. C. Weston, *US Pat*, 2000, 6049018.
- 30 S. Inagaki, K. Takechi and Y. Kubota, *Chem. Commun.*, 2010, **46**, 2662.
- 31 Y. Kubota, S. Inagaki and K. Takechi, *Catal. Today*, 2014, **226**, 109.
- 32 S. Park, Y. Watanabe, Y. Nishita, T. Fukuoka, S. Inagaki and Y. Kubota, *J. Catal.*, 2014, **319**, 265.
- 33 Y. Kubota and S. Inagaki, *Top. Catal.*, 2015, **58**, 480.
- 34 J. G. Moscoso and D. Y. Jan, *US Pat*, 2011, 7922997.
- 35 S. Inagaki, Y. Tsuboi, Y. Nishita, T. Syahylah, T. Wakihara and Y. Kubota, *Chem. – Eur. J.*, 2013, **19**, 7780.
- 36 Y. Kubota, K. Itabashi, S. Inagaki, Y. Nishita, R. Komatsu, Y. Tsuboi, S. Shinoda and T. Okubo, *Chem. Mater.*, 2014, **26**, 1250.
- 37 Y. Kubota, S. Inagaki, Y. Nishita, K. Itabashi, Y. Tsuboi, T. Syahylah and T. Okubo, *Catal. Today*, 2015, **243**, 85.
- 38 T. Ikeda, S. Inagaki, T. Hanaoka and Y. Kubota, *J. Phys. Chem. C*, 2010, **114**, 19641.
- 39 Y. Koyama, T. Ikeda, T. Tatsumi and Y. Kubota, *Angew. Chem., Int. Ed.*, 2008, **47**, 1042.
- 40 W. Fan, R.-G. Guan, T. Yokoi, P. Wu, Y. Kubota and T. Tatsumi, *J. Am. Chem. Soc.*, 2008, **130**, 10150 and references cited therein.
- 41 M. Taramasso, G. Perego and B. Notari, *US Pat*, 1983, 4410501.